



¹⁸F-RGD PET/CT imaging reveals characteristics of angiogenesis in non-small cell lung cancer

Li Li^{1,2,3}, Wei Zhao², Xiaorong Sun⁴, Ning Liu², Yue Zhou⁵, Xiaohui Luan⁶, Song Gao⁷, Shuqiang Zhao⁴, Jinming Yu^{2,3,8}, Shuanghu Yuan^{2,3,8}

¹Shandong First Medical University and Shandong Academy of Medical Sciences, Jinan, China; ²Department of Radiation Oncology, Shandong Cancer Hospital and Institute, Shandong First Medical University and Shandong Academy of Medical Sciences, Jinan, China; ³Department of Radiation Oncology, Shandong Cancer Hospital and Institute-Shandong Cancer Hospital Affiliated to Shandong First Medical University, Jinan, China; ⁴Department of Nuclear Medicine, Shandong Cancer Hospital and Institute, Shandong First Medical University and Shandong Academy of Medical Sciences, Jinan, China; ⁵Department of Oncology, Shanghe People's Hospital, Jinan, China; ⁶Department of Radiation Oncology, Dezhou People's Hospital, Dezhou, China; ⁷Department of Oncology, Jining Infectious Diseases Hospital, Jining, China; ⁸Cheeloo College of Medicine, Shandong University, Jinan, China

Contributions: (I) Conception and design: S Yuan, L Li; (II) Administrative support: S Yuan, J Yu; (III) Provision of study materials or patients: S Yuan, J Yu, L Li; (IV) Collection and assembly of data: L Li, N Liu, Y Zhou, X Luan, S Gao; (V) Data analysis and interpretation: L Li, W Zhao, X Sun, S Zhao; (VI) Manuscript writing: All authors; (VII) Final approval of manuscript: All authors.

Correspondence to: Shuanghu Yuan, MD, PhD. Department of Radiation Oncology, Shandong Cancer Hospital and Institute, Shandong First Medical University and Shandong Academy of Medical Sciences, No 440 Jiyuan Road, Jinan 250117, China. Email: yuanshuanghu@sina.com.

Background: The objective of this study was to explore the benefit of ¹⁸F-AIF-NOTA-PRGD2 positron emission tomography/computed tomography (denoted as ¹⁸F-RGD PET/CT) imaging for determining the clinical pathologic features of non-small cell lung cancer (NSCLC).

Methods: Seventy-two patients with NSCLC (37 cases of adenocarcinoma and 35 cases of squamous carcinoma) were enrolled to receive ¹⁸F-RGD PET/CT scanning pretreatment. The peak standard uptake value (SUV_{peak}), mean standard uptake value (SUV_{mean}), angiogenic tumor volume (ATV) and total lesion angiogenesis (TLA) of tumors were determined using an automated contouring program. Cases were classified according to the tumor, lymph node, metastasis (TNM) stage.

Results: Significant differences in ATV and TLA were observed among T1, T2, T3 and T4 cases (ATV, P=0.000; TLA, P=0.000). ATV and TLA also differed significantly among cases of clinical stage I, II, III and IV (ATV, P=0.002; TLA, P=0.011). However, no significant differences in any values were observed between stage III and IV NSCLC cases (SUV_{peak}, P=0.675; SUV_{mean}, P=0.668; ATV, P=0.52; TLA, P=0.634). All assessed values were higher in squamous cell carcinoma cases than in adenocarcinoma cases (SUV_{peak}, P=0.045; SUV_{mean}, P=0.014; ATV, P=0.003; TLA, P=0.001). For clinical stage III and IV cases specifically, SUV_{peak}, SUV_{mean} and TLA were higher for squamous cell carcinoma than for adenocarcinoma (SUV_{peak}, P=0.015; SUV_{mean}, P=0.009; TLA, P=0.036).

Conclusions: ¹⁸F-RGD PET/CT imaging revealed the presence of increased angiogenesis in the tumor microenvironment of NSCLC, especially squamous cell carcinoma, and thus may be valuable in planning therapeutic regimens for individual patients.

Keywords: ¹⁸F-RGD PET/CT; angiogenesis; characteristics; non-small cell lung cancer (NSCLC)

Submitted Jan 31, 2020. Accepted for publication Jul 03, 2020.

doi: 10.21037/tlcr-20-187

View this article at: <http://dx.doi.org/10.21037/tlcr-20-187>

Introduction

Lung cancer is the most common cause of cancer-related death worldwide, with a 5-year survival rate from diagnosis of only approximately 18% (1). Generally, accurate pathological diagnosis and the tumor, lymph node, metastasis (TNM) stage are particularly important for the development of individualized treatment strategies. Concurrent chemotherapy/radiotherapy (CCRT) is recommended as the first-line treatment for patients with inoperable stage II (node positive) and stage III non-small cell lung cancer (NSCLC) (2). With the continued development of novel agents targeting specific mutations or pathways associated with angiogenic mechanisms, promising clinical benefits are driving the acceptance of these therapies as first-line choices rather than third-line in cancer treatment (2). However, the curative effects of CCRT, targeted therapy, and antiangiogenic therapy vary even among the NSCLC cases of the same TNM stage (3-5). Therefore, new parameters representing the clinical features of NSCLC are needed in order to identify populations that will be responsive to specific treatments.

Neovascularization, one important component of the tumor microenvironment (TME), is often highly abnormal and heterogeneous within tumors. It is the basis of tumor proliferation, invasion, recurrence and metastasis (6). The process of angiogenesis is a pathological situation in which new capillaries sprout from existing vessels primarily composed of endothelial cells (7,8). Functional and structural angiogenic abnormalities can lead to impaired tissue perfusion, directly resulting in a hypoxic TME and fueling tumor progression and treatment resistance (9-11). From this perspective, angiogenesis-based *in vivo* imaging could be a valuable clinical tool for noninvasive evaluation of the TME. High expression of integrin $\alpha v\beta 3$ in activated endothelial cells make this protein a potential surrogate parameter for angiogenesis in tumors (12,13). As the tripeptide moiety of arginine-glycine-aspartate (RGD) interacts specifically with integrin $\alpha v\beta 3$ and exhibits a significant positive correlation with $\alpha v\beta 3$ expression, RGD-based molecular imaging intuitively represents a potentially feasible imaging approach for assessing angiogenesis with the TME (14-16).

Our previous study demonstrated that ^{18}F -ALF-NOTA-PRGD2 can be used to characterize tumor angiogenesis clearly (17). However, that study only analysed the correlation between RGD uptake values and the antiangiogenic effect in 28 pan-cancer patients, including

only 9 lung cancer patients. To better demonstrate the biological characteristics of NSCLC, the present study was carried out to explore the correlation between the angiogenic status and clinical pathologic features of NSCLC using ^{18}F -ALF-NOTA-PRGD2 positron emission tomography/computed tomography (denoted as ^{18}F -RGD PET/CT) imaging.

We present the following article in accordance with the STROBE reporting checklist (available at <http://dx.doi.org/10.21037/tlcr-20-187>).

Methods

Our investigation of 72 patients was performed in accordance with the Declaration of Helsinki (as revised in 2013) and approved by the Ethical Committee of Shandong Cancer Hospital and Institute (No. SDTHEC20130326). All patients provided written consent for participation in this study.

Patients

Patients with cytologically or histologically confirmed NSCLC were prospectively enrolled and underwent ^{18}F -RGD PET/CT scanning at baseline at the Shandong Cancer Hospital and Institute.

^{18}F -RGD PET/CT scanning

A lyophilized kit for labeling the PRGD2 peptide (Jiangsu Institute of Nuclear Medicine) was used according to the previously published protocol (18). No fasting or specific CT contrast agents were needed. PET scans were performed 60 min after intravenous injection of ^{18}F -RGD at approximately 1.89 ± 0.37 MBq/kg. The PET scans were acquired on a combined PET/CT scanner (GEMINI TF Big Bore; Philips Healthcare) for 5 min per field of view. A low-dose CT scan for attenuation-correction and localization purposes was also acquired. The patients were advised to remain motionless and to breathe shallowly during the examination.

Imaging data processing

All the PET and CT imaging data were transferred into MIM software (MIM, 6.1.0, Cleveland, OH, USA). The radiotracer concentration in the regions of interest (ROIs)

Table 1 Characteristics of included patients

Characteristics	Outcome
Age (years), median (range)	60 (44–85)
Gender, n	
Female	20
Male	52
Smoking, n	
Yes	46
No	26
KPS, median (range)	85 (70–100)
Pathological subtype, n	
Adenocarcinoma	37
Squamous carcinoma	35
Clinical stage, n	
I	7
II	7
III	45
IV	13
Greatest dimension, n	
≤3 cm	28
3–5 cm	26
5–7 cm	13
>7 cm	5

was normalized to the injected dose per kilogram of the patients' body weight to derive the standardized uptake values (SUVs). ROIs were drawn on transverse slices of the PET scanning images with reference to the CT slices by experienced nuclear medicine physicians, and the MIM software would directly delineate the target tumor with a drawing threshold of 40% (maximum SUV) SUV_{max} . The peak SUV (SUV_{peak}), mean SUV (SUV_{mean}), angiogenic tumor volume (ATV) and total lesion angiogenesis (TLA) were also calculated automatically. The TLA represented the product of SUV_{mean} and ATV.

Measurement of tumor size

The greatest dimension of the primary tumor was obtained

on CT images by two experienced nuclear medicine physicians. The greatest dimension was classified as T1 (dimension ≤3 cm), T2 (3 cm < dimension ≤5 cm), T3 (5 cm < dimension ≤7 cm) or T4 (dimension >7 cm), referring to the definitions for T, N, and M in the National Comprehensive Cancer Network guidelines (2).

Statistical analysis

Statistical analyses were performed using SPSS 20.0 statistical software (SPSS Inc., Chicago, IL, USA). Imaging parameters were compared between cases according to clinical TNM stages and pathologic types using independent-samples *t*-test, Mann-Whitney U test or one-way analysis of variance (ANOVA), and associations between imaging parameters and clinical TNM stage and pathologic type were determined by Spearman or Pearson correlation analysis. Probability values less than 0.05 were considered statistically significant.

Results

From July 2013 to March 2019, 72 patients diagnosed with NSCLC based on cytology or histological examinations at Shandong Cancer Hospital and Institute were enrolled in the study. The patients' characteristics are presented in *Table 1*.

Relationships between ^{18}F -RGD PET/CT imaging parameters and greatest tumor dimension

The SUV_{peak} , SUV_{mean} , ATV and TLA were positively correlated with greatest tumor dimension (SUV_{peak} , $r=0.234$, $P=0.048$; SUV_{mean} , $r=0.241$, $P=0.042$; ATV, $r=0.595$, $P=0.000$; TLA, $r=0.584$, $P=0.000$). ATV and TLA were found to differ significantly among tumors of the T1, T2, T3 and T4 size categories (ATV, 17.45 ± 17.71 , 37.67 ± 24.27 , 69.37 ± 53.14 and 107.62 ± 50.57 , respectively, $P=0.000$; TLA, 38.10 ± 30.52 , 109.85 ± 75.81 , 240.95 ± 225.01 and 430.31 ± 334.26 , respectively, $P=0.000$), whereas no significant differences in SUV_{peak} and SUV_{mean} were found among the T1, T2, T3 and T4 categories (SUV_{peak} , 3.69 ± 1.83 , 4.63 ± 1.90 , 4.99 ± 2.66 and 5.54 ± 2.45 , respectively, $P=0.215$; SUV_{mean} , 2.54 ± 1.23 , 3.06 ± 1.37 , 3.27 ± 1.76 and 3.60 ± 1.65 , respectively, $P=0.315$) (*Figure 1*). Overall, the ATV and TLA values increased significantly with increasing

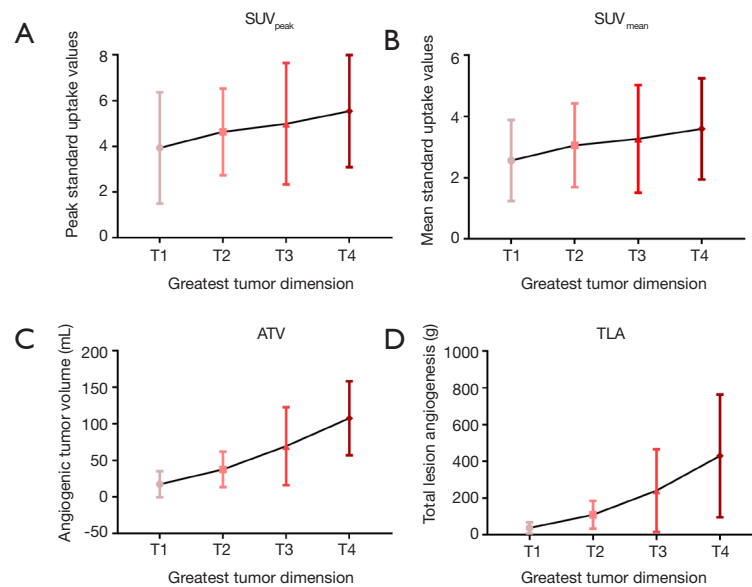


Figure 1 ^{18}F -RGD PET/CT imaging parameters according to different categories of greatest tumor dimension.

tumor diameter.

Relationships between ^{18}F -RGD PET/CT imaging parameters and clinical stage

Significant increases in ATV and TLA were seen with advancing clinical stage from I to IV (ATV, $r=0.378$, $P=0.001$; TLA, $r=0.313$, $P=0.008$). Moreover, the ATV and TLA values differed significantly among clinical stage I+II, stage III and stage IV (ATV, $P=0.002$; TLA, $P=0.011$) (Table 2, Figure 2). However, no significant differences in any of the imaging parameters (SUV_{peak} , SUV_{mean} , ATV and TLA) were found between clinical stage III and IV (SUV_{peak} , $P=0.675$; SUV_{mean} , $P=0.668$; ATV, $P=0.52$; TLA, $P=0.634$).

Relationships between ^{18}F -RGD PET/CT imaging parameters and pathological subtype

Significantly higher SUV_{peak} , SUV_{mean} , ATV and TLA values on ^{18}F -RGD PET/CT imaging were seen for squamous carcinoma as compared to adenocarcinoma ($P=0.045$, $P=0.014$, $P=0.003$ and $P=0.001$, respectively) (Table 3, Figure 3). For clinical stage III and IV NSCLC specifically, all imaging parameters were higher in squamous carcinoma cases than in adenocarcinoma cases (SUV_{peak} , 4.98 ± 2.44 vs. 3.69 ± 1.46 , $P=0.015$; SUV_{mean} , 3.34 ± 1.66 vs. 2.41 ± 0.93 , $P=0.009$; 50.36 ± 40.50 vs. 42.15 ± 44.94 , $P=0.111$; TLA,

186.90 ± 212.40 vs. 99.81 ± 125.73 , $P=0.036$; Figure 4).

Discussion

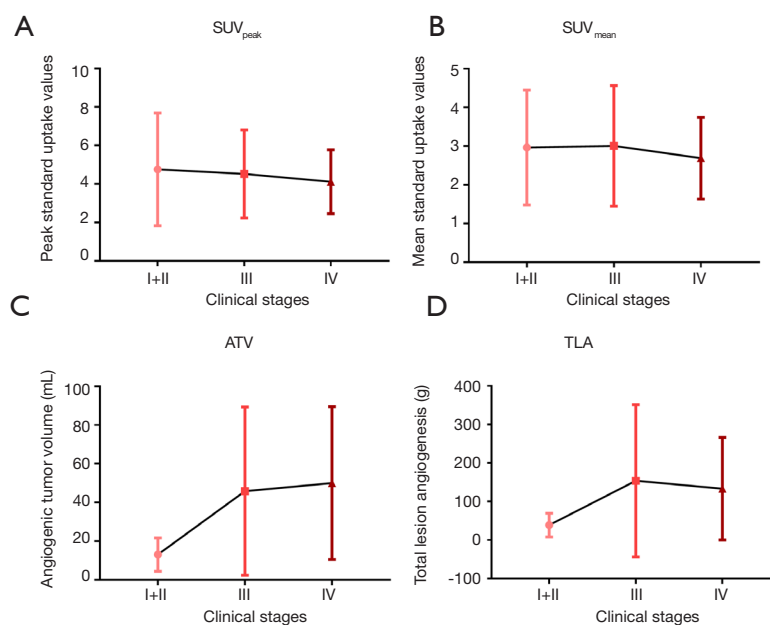
In support of the development of personalized precision medicine, it is very important to characterize the clinical pathological heterogeneity of lung cancer among patients. The results of our current study provide clinical evidence that ^{18}F -RGD PET/CT imaging parameters correlate significantly with the greatest tumor dimension, clinical stage and pathological subtype of NSCLC, with higher SUVs correlating with later stage squamous carcinoma and larger tumor diameter.

Several studies have demonstrated advantages of RGD-based imaging over fluorodeoxyglucose (FDG)-based imaging. Wei *et al.* conducted micro-PET imaging in Lewis lung carcinoma-bearing C57BL/6 mice using both imaging modalities, and the sensitivity, specificity, and accuracy of ^{18}F -RGD PET/CT for identifying necrotic tumor area and metabolic tumor volume (MTV) were higher than those of ^{18}F -FDG PET/CT (19). Additional clinical studies also reported advantages of RGD-based imaging over FDG-based PET/CT, showing that ^{18}F -RGD PET/CT is more sensitive and applicable for evaluating the heterogeneity of the TME, especially as associated with integrin $\alpha\text{V}\beta 3$ expression or angiogenesis (20,21). Previous studies primarily focused on evaluating the heterogeneity

Table 2 Relationships between ^{18}F -RGD PET/CT imaging parameters and clinical staging

Parameters	TNM stage			P
	I+II	III	IV	
SUV _{peak}	4.37±1.99	4.52±2.29	4.11±1.66	0.882
SUV _{mean}	2.97±1.32	3.01±1.56	2.69±1.06	0.881
ATV	13.10±8.64	45.90±43.44	50.03±39.50	0.002
TLA	38.91±30.85	153.98±197.38	133.38±133.05	0.011

ATV, angiogenic tumor volume; TLA, total lesion angiogenesis.

**Figure 2** ^{18}F -RGD PET/CT imaging parameters according to different clinical stages of NSCLC.

between NSCLC and SCLC using RGD PET/CT imaging (20,21). Kang *et al.* showed that NSCLC had higher ⁽⁶⁸⁾Ga-RGD uptake values than SCLC and was unlikely to benefit from anti-angiogenic therapy (22). However, until now, no clinical studies have explored the heterogeneity of angiogenic status in NSCLC.

The present study mainly focused on intra-tumor TME heterogeneity in patients with NSCLC on the basis of recognized clinical staging. It is well known that additional neovascularization is needed for adequate nutrient transfer as the tumor diameter increases, especially beyond a volume of 2 mm³ (23). Our results revealed a significant positive correlation between the greatest tumor dimension and RGD uptake values. This trend demonstrated that our

imaging parameters are reflective of the true dimension of the tumor, and thus, RGD PET/CT could be valuable tool for assessing the TME.

The ATV and TLA values were higher for stage III or IV NSCLC cases than for stage I and II cases, and this result was similar with findings in glioma, in which RGD uptake values also showed positive correlation with World Health Organization (WHO) grading (21,24). However, we found no statistically significant differences in RGD uptake parameters between stage III and IV cases. Notably, the RGD uptake parameters SUV_{peak}, SUV_{mean} and TLA were all significantly higher for squamous cell carcinoma than for adenocarcinoma, even among stage III and IV NSCLC cases. Based on these data, we propose that the

Table 3 Relationships between ¹⁸F-RGD PET/CT imaging parameters and pathological subtype of NSCLC

Parameters	Pathological subtype		P
	Squamous carcinoma	Adenocarcinoma	
SUV _{peak}	5.05±2.40	3.96±2.10	0.045
SUV _{mean}	3.37±1.63	2.53±1.14	0.014
ATV	48.99±39.77	33.09±40.53	0.003
TLA	181.77±207.19	79.10±110.95	0.001

NSCLC, non-small cell lung cancer; ATV, angiogenic tumor volume; TLA, total lesion angiogenesis.

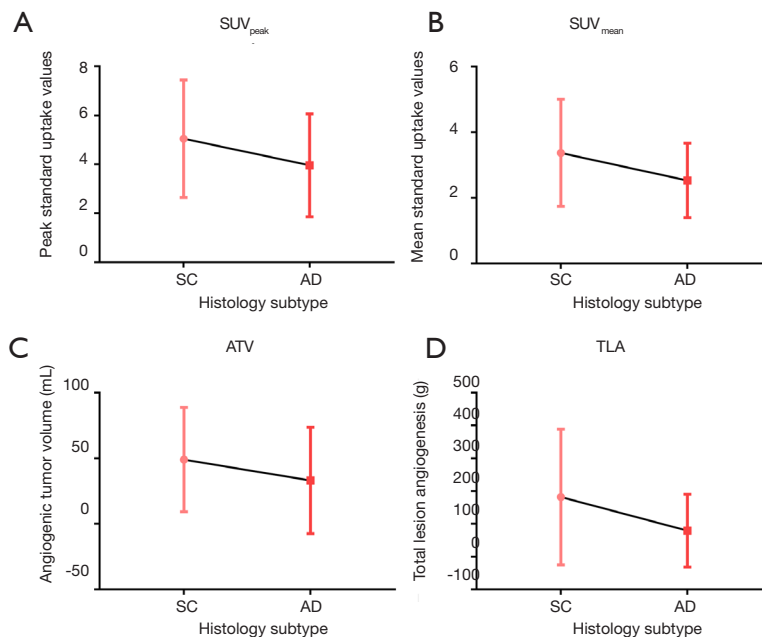


Figure 3 ¹⁸F-RGD PET/CT imaging parameters according to different pathological subtype of NSCLC. SC, squamous carcinoma; AD, adenocarcinoma.

parameters obtained by ¹⁸F-RGD PET can reflect the TME heterogeneity effectively and, as such, may offer a certain comparative advantage over traditional TNM staging.

In our study, the ATV and TLA values were significantly greater in cases of squamous cell carcinoma, implying that neovascularization in squamous carcinoma may be more abundant than that in adenocarcinoma. Our original study revealed the phenomenon that higher RGD uptake values are associated with better responses to antiangiogenic therapy in preclinical and clinical studies (17,25), suggesting that squamous carcinoma may have a better therapeutic effect in antiangiogenic therapy. Certainly, researchers should not only focus on the treatment efficacy, but also pay

attention to the safety management in clinical applications. It is still an essential step to assess the risk of bleeding during clinical decision-making for individual patients.

Additionally, the higher RGD uptake values could predict the poor efficacy of chemoradiotherapy in locally advanced NSCLC, which may result from the hypoxic TME and treatment resistance caused by nonfunctional tumor neovascularization (9-11,26). In general, ¹⁸F-RGD PET/CT molecular imaging related to αVβ₃ expression provides a tool for assessing tumor heterogeneity and thus offers predictive value for personalized tumor therapy. Further studies with larger cohorts of NSCLC patients and related subgroup analyses are warranted to investigate this

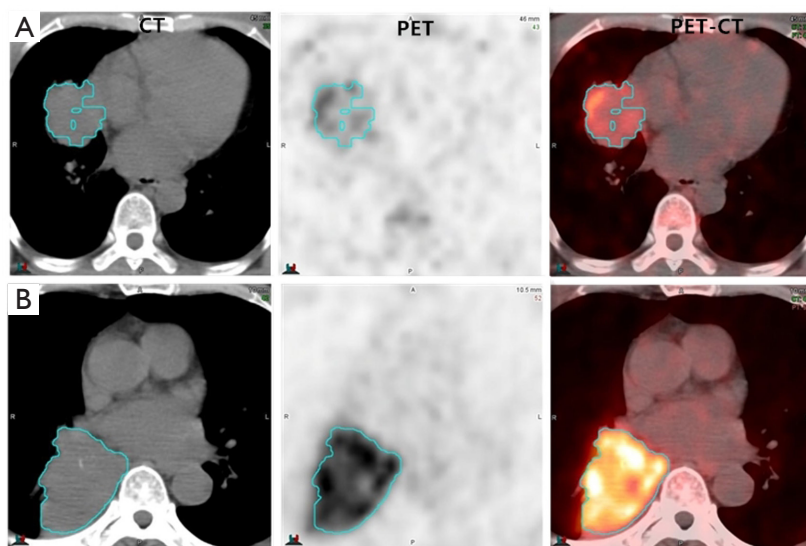


Figure 4 Representative ^{18}F -RGD PET/CT scans of adenocarcinoma with low RGD uptake values (A, $\text{SUV}_{\text{peak}}=1.68$, $\text{SUV}_{\text{mean}}=1.13$, $\text{ATV}=77.92$, $\text{TLA}=87.71$) and squamous carcinoma with high RGD uptake values (B, $\text{SUV}_{\text{peak}}=8.58$, $\text{SUV}_{\text{mean}}=5.80$, $\text{ATV}=163.42$, $\text{TLA}=947.72$).

possibility.

Conclusions

The TME of NSCLC with a large dimension and advanced clinical stage, especially squamous cell carcinoma, is more likely to present extensive angiogenesis, and related parameters on ^{18}F -RGD PET/CT imaging can be applied in the planning of appropriate therapeutic regimens.

Acknowledgments

Funding: This study was partially funded by the Natural Science Foundation of China (NSFC81872475, NSFC81372413), the Shandong Key Research and Development Plan (2017CXGC1209 and 2017GSF18164), the Outstanding Youth Natural Science Foundation of Shandong Province (JQ201423), the Jinan Clinical Medicine Science and Technology Innovation Plan (201704095), and the National Key Research and Development Program of China (2016YFC0904700).

Footnote

Reporting Checklist: The authors have completed the

STROBE reporting checklist. Available at <http://dx.doi.org/10.21037/tlcr-20-187>

Data Sharing Statement: Available at <http://dx.doi.org/10.21037/tlcr-20-187>

Conflicts of Interest: All authors have completed the ICMJE uniform disclosure form (available at <http://dx.doi.org/10.21037/tlcr-20-187>). The authors have no conflicts of interest to declare.

Ethical Statement: The authors are accountable for all aspects of the work in ensuring that questions related to the accuracy or integrity of any part of the work are appropriately investigated and resolved. Our investigation of 72 patients was performed in accordance with the Declaration of Helsinki (as revised in 2013) and approved by the Ethical Committee of Shandong Cancer Hospital and Institute (No. SDTHEC20130326). All patients provided written consent for participation in this study.

Open Access Statement: This is an Open Access article distributed in accordance with the Creative Commons Attribution-NonCommercial-NoDerivs 4.0 International License (CC BY-NC-ND 4.0), which permits the non-

commercial replication and distribution of the article with the strict proviso that no changes or edits are made and the original work is properly cited (including links to both the formal publication through the relevant DOI and the license). See: <https://creativecommons.org/licenses/by-nc-nd/4.0/>.

References

1. Ferlay J, Soerjomataram I, Dikshit R, et al. Cancer incidence and mortality worldwide: sources, methods and major patterns in GLOBOCAN 2012. *Int J Cancer* 2015;136:E359-86.
2. NCCN Clinical Practice Guidelines in Non-Small Cell Lung Cancer (NCCN Guidelines). Available online: https://www.nccn.org/professionals/physician_gls/pdf/nscl.pdf
3. Auperin A, Le PC, Rolland E, et al. Meta-analysis of concomitant versus sequential radiochemotherapy in locally advanced non-small-cell lung cancer. *J Clin Oncol* 2010;28:2181-90.
4. Zer A, Leighl NB. Second-line therapy in non-small-cell lung cancer: the DELTA between different genotypes widens. *J Clin Oncol* 2014;32:1874-81.
5. Liu Z, Ou W, Li N, et al. Apatinib monotherapy for advanced non-small cell lung cancer after the failure of chemotherapy or other targeted therapy. *Thorac Cancer* 2018;9:1285-90.
6. Carmeliet P. Angiogenesis in health and disease. *Nat Med* 2003;9:653-60.
7. Risau W. Differentiation of endothelium. *FASEB J* 1995;9:926-33.
8. Hanahan D, Folkman J. Patterns and emerging mechanisms of the angiogenic switch during tumorigenesis. *Cell* 1996;86:353-64.
9. Shweiki D, Itin A, Soffer D, et al. Vascular endothelial growth factor induced by hypoxia may mediate hypoxia-initiated angiogenesis. *Nature* 1992;359:843-5.
10. Jain RK. Normalizing tumor microenvironment to treat cancer: bench to bedside to biomarkers. *J Clin Oncol* 2013;31:2205-18.
11. Jain RK. Antiangiogenesis strategies revisited: from starving tumors to alleviating hypoxia. *Cancer Cell* 2014;26:605-22.
12. Liu Z, Wang F, Chen X. Integrin alpha(v)beta(3)-Targeted Cancer Therapy. *Drug Dev Res* 2008;69:329-39.
13. Kumar CC. Integrin alpha v beta 3 as a therapeutic target for blocking tumor-induced angiogenesis. *Curr Drug Targets* 2003;4:123-31.
14. Yu YP, Wang Q, Liu YC, et al. Molecular basis for the targeted binding of RGD-containing peptide to integrin alphaVbeta3. *Biomaterials* 2014;35:1667-75.
15. Beer AJ, Haubner R, Sarbia M, et al. Positron emission tomography using [18F]Galacto-RGD identifies the level of integrin alpha(v)beta3 expression in man. *Clin Cancer Res* 2006;12:3942-9.
16. Iagaru A, Gambhir SS. Imaging tumor angiogenesis: the road to clinical utility. *AJR Am J Roentgenol* 2013;201:W183-91.
17. Li L, Ma L, Shang D, et al. Pretreatment PET/CT imaging of angiogenesis based on (18)F-RGD tracer uptake may predict antiangiogenic response. *Eur J Nucl Med Mol Imaging* 2019;46:940-7.
18. Wan W, Guo N, Pan D, et al. First experience of 18F-alfatide in lung cancer patients using a new lyophilized kit for rapid radiofluorination. *J Nucl Med* 2013;54:691-8.
19. Wei YC, Hu X, Gao Y, et al. Noninvasive Evaluation of Metabolic Tumor Volume in Lewis Lung Carcinoma Tumor-Bearing C57BL/6 Mice with Micro-PET and the Radiotracers 18F-Alfatide and 18F-FDG: A Comparative Analysis. *PLoS One* 2015;10:e0136195.
20. Beer AJ, Lorenzen S, Metz S, et al. Comparison of integrin alphaVbeta3 expression and glucose metabolism in primary and metastatic lesions in cancer patients: a PET study using 18F-galacto-RGD and 18F-FDG. *J Nucl Med* 2008;49:22-9.
21. Li D, Zhao X, Zhang L, et al. (68)Ga-PRGD2 PET/CT in the evaluation of Glioma: a prospective study. *Mol Pharm* 2014;11:3923-9.
22. Kang F, Wang Z, Li G, et al. Inter-heterogeneity and intra-heterogeneity of alphavbeta3 in non-small cell lung cancer and small cell lung cancer patients as revealed by (68)Ga-RGD2 PET imaging. *Eur J Nucl Med Mol Imaging* 2017;44:1520-8.
23. Abdelrahim M, Konduri S, Basha R, et al. Angiogenesis: an update and potential drug approaches (review). *Int J Oncol* 2010;36:5-18.
24. Liu N, Zhao W, Hu X, et al. A pilot study on imaging of integrin $\alpha v \beta 3$ with RGD PET in patients with glioma. *J Nucl Med* 2015;56:324.

25. Liu J, Wang D, Meng X, et al. ^{18}F -alfatide positron emission tomography may predict antiangiogenic responses. *Oncol Rep* 2018;40:2896-905.
26. Luan X, Huang Y, Gao S, et al. (^{18}F) -alfatide PET/

CT may predict short-term outcome of concurrent chemoradiotherapy in patients with advanced non-small cell lung cancer. *Eur J Nucl Med Mol Imaging* 2016;43:2336-42.

Cite this article as: Li L, Zhao W, Sun X, Liu N, Zhou Y, Luan X, Gao S, Zhao S, Yu J, Yuan S. ^{18}F -RGD PET/CT imaging reveals characteristics of angiogenesis in non-small cell lung cancer. *Transl Lung Cancer Res* 2020;9(4):1324-1332. doi: 10.21037/tlcr-20-187